Decay and diffusion characteristic of electron and ion surface charges on MgO

Ho Jung Syn, Dong Cheol Jeong*, Tae Ho Lee, and Ki Woong Whang
School of Electrical Engineering and Computer Science, Seoul National Univ.
San 56-1, Shillim-dong, Kwanak-ku, Seoul, Korea
Phone: 82-2-880-9554, E-mail: hjsyn@pllab.snu.ac.kr
*** Department of Display Engineering, Hoseo University, Asan-city, Chungcheongnam-do, 336-795, Korea**

Keywords : MgO, Diffusion, Decay

Abstract

In this work, we measured the spatiotemporal surface charge distribution by the longitudinal electro-optic amplitude modulation method with BSO single crystal to investigate the decay and diffusion characteristics of surface charges in three types of MgO. The speed of decay and diffusion of two different kinds doped MgO is compared with those of pure MgO. The difference in the characteristics of the decay and diffusion between the electron and ion surface charges is investigated separately. We found that the rate of ion decay is the major factor that makes the difference of the temporal variation of wall voltage among different types doped MgO.

1. Introduction

The alternating current plasma display panel (ac PDP) has been one of the major flat panel display device owing to high image quality and easily making large size panel at economical price. Recently, there is a strong request to make ac PDP for full high definition(1920 x 1080) TV with lower cost and consumed power. It is recently suggested doping MgO with a diversity of materials in order to improve addressing delay time. [1] It have been already studied that the impurity doping into the MgO thin film affected surface charge movements on MgO such as decay and diffusion due to the change of electrical conductivity. [2] In this research, we classified decay and diffusion from the spatiotemporal change of surface charge distribution which was investigated by longitudinal electro-optic amplitude modulation with $Bi_{12}SiO_{20}$(BSO) single crystal. We separated the diffusion from decay by analyzing in the horizontal and vertical direction, respectively and obtained the decay time constants and diffusion coefficients of MgO with different type of dopants.

2. Experimental

We had to measure the spatiotemporal surface charge distribution on MgO prior to analyzing both the diffusion and decay behavior. It was reported that the wall charge measurement could be made by using the longitudinal electro optic amplitude modulation method with $Bi_{12}SiO_{20}$(BSO) single crystal in ac PDP. [3] To normalize the spatiotemporal surface charge distribution for analyzing diffusion and decay effectively, the discharge cell was designed to have a counter discharge structure in order to form the surface charge similar to Gaussian distribution. Fig. 1 shows the schematic diagram of cell structure used in this experiment. The cell size was 2 x 2 mm, and barrier rib height was 200 μm. The electrode width was 200 μm and the dielectric thickness of rear panel was 35 μm. BSO which had thickness of 120 μm was used as the dielectric in front panel. Lastly, MgO layer with thickness of 450nm was deposited by electron beam evaporation on both sides. Finally the test sample was loaded in the chamber which is filled with Ne-4% Xe at 100 torr. Fig. 2 presents waveforms to make counter discharge. To observe the change of surface charge distribution adequately, we gave long pause time, 1ms. The starting point of measurement was after 24 μs from the pulse off time well separated from the self-erase discharge.

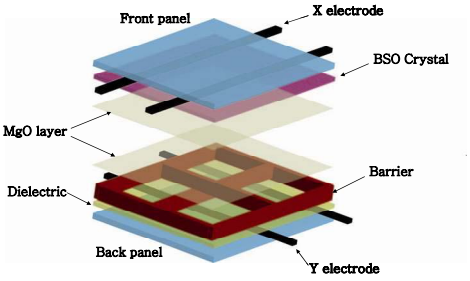

Fig. 1 Schematics of cell structure.

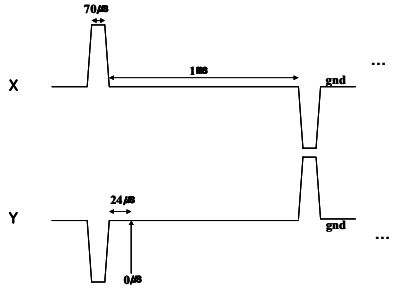

Fig. 2 Driving voltage waveform applied to X and Y electrode.

To compare with the different characteristics of surface charge decrement as different types of MgO, we used MgO with three different types of dopants. Above all, pure MgO (Mitsubishi

Material Co., 99.9%, sintered type) was used for reference. Second, MgO was co-doped with Sc and Al and it would be called MgO1 in this paper. Third, MgO was additionally co-doped with Ca in MgO1 and it would be called MgO2.

3. Results and discussion

3.1 Diffusion coefficient

In order to distinguish the decay and diffusion behavior, we analyzed the surface charge in the two different directions. Through the observation of the surface charge in the horizontal direction and vertical direction, we could calculate the diffusion coefficient and decay time constant, respectively. First of all, to calculate the diffusion coefficient, after Gaussian fitting we calculated the degree of temporal variation of Gaussian width which had information on the spreading speed. Fig. 3 (a) shows the surface charge distributions and Gaussian fitted functions of electron surface charge and Fig. 3 (b) also shows those of ion surface charge on pure MgO. The distribution could be fitted by the following equation.

$$y(x) = y_0 + \frac{Q}{w \cdot \sqrt{\pi/2}} \exp[-\frac{2(x-x_0)^2}{w^2}] \quad (1)$$

After normalizing into Gaussian function, we could calculate the diffusion coefficient from the change of Gaussian width, w^2, with time. From the solution of Fick's second Law given by equation (2).

$$\sigma(x,t) = \frac{Q}{\sqrt{\pi Dt}} \exp[-\frac{x^2}{4Dt}] \quad (2)$$

We could relate the diffusion coefficient, D, and Gaussian width, w^2 as, [4]

$$D \approx \frac{d}{dt}\frac{w^2}{8} \quad (3)$$

Fig. 4 (a) and (b) show the temporal change of $w^2/8$ and linear fitting curve of ion and electron surface charge on pure MgO, respectively. We could obtain the diffusion coefficients of ion and electron as follows:

$$D_{ION} \approx 6.80\times10^{-6} m^2/\text{sec}, \quad D_{ELEC} \approx 9.12\times10^{-5} m^2/\text{sec}$$

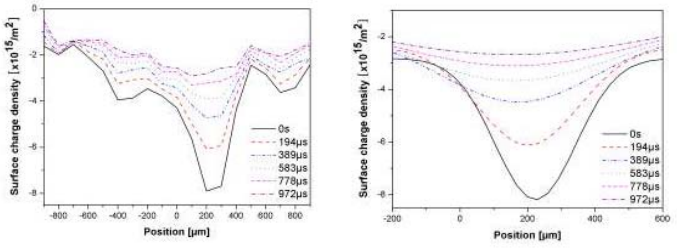

(a)

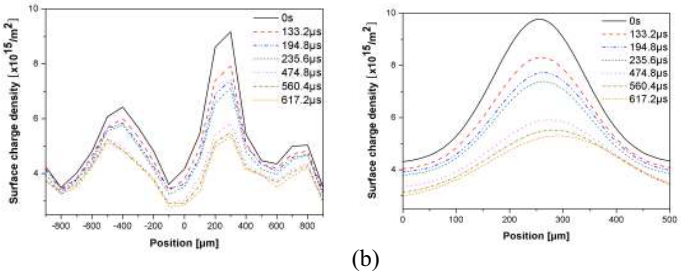

(b)

Fig. 3 Spatiotemporal surface distribution and Gaussian fitted curves of pure MgO: (a) electron and (b) ion surface charge.

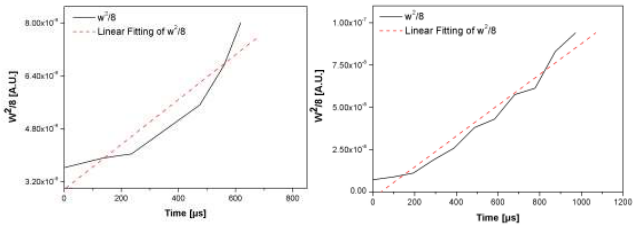

(a) (b)

Fig. 4 Temporal variation of $w^2/8$ and linearly fitted curves of pure MgO: (a) ion and (b) electron surface charge.

3.2 Decay time constant

The decrement of peak density due to diffusion was different from the decrement of peak density observed value at a particular time implies that there is also a pure decay.

Graph (1) and graph (4) in Fig. 5 represent surface charge distribution fitted into Gaussian function of electron surface charge on pure MgO at 0 μs and 292 μs, respectively. Equation (4) and (5) describe the Gaussian fitted equations at 0 μs and 292 μs, respectively. The w_i at 0 μs and 292 μs were w_1 and w_2, respectively.

$$y_1(x) = y_{01} + \frac{Q_{01}}{\sqrt{\pi w_i^{\,2}/2}} \exp[-\frac{x^2}{w_i^{\,2}/2}], \qquad w_i = w_1 \quad (4)$$

$$y_2(x) = y_{02} + \frac{Q_{02}}{\sqrt{\pi w_i^{\,2}/2}} \exp[-\frac{x^2}{w_i^{\,2}/2}], \qquad w_i = w_2 \quad (5)$$

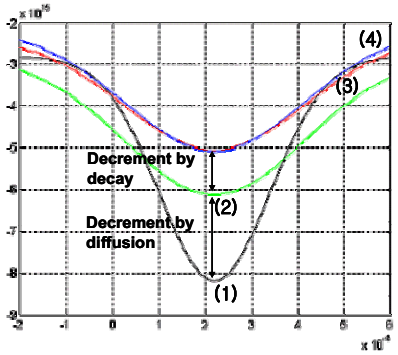

Fig. 5 Classify the decrement of peak value by decay and diffusion.

The four Graphs in Fig. 5 represent as follows:

$y_1\big|_{t=0\mu s,\ w_i=w_1}$ Graph (1)

$y_1\big|_{w_i=w_2}$ Graph (2)

$Ay_1\big|_{w_i=w_2,\ A=0.83}$ $0 < A \le 1$ Graph (3)

$y_2\big|_{t=292\mu s,\ w_i=w_2}$ Graph(4)

For taking the decrement of peak density caused by diffusion during 292 μs, w_1 of equation (4) was replaced by w_2 to be Graph(2). Because the decrement of peak density by pure diffusion was caused by change of w_i, the difference of peak value between Graph (1) and Graph (2) implied the decrement of peak density owing to diffusion, exclusively. Nevertheless, the peak value of Graph(2) did not accord with that of Graph(4). Assuming that the decrement rate of all positions was the same, we multiplied Graph(2) by A for the peak value of Graph(2) corresponded with that of Graph(4). The A meant the ratio of decrement of peak value from initial value only due to decay. We could make equation (6) considered both diffusion and decay.

$$\sigma(x,t) = A(t) \cdot [y_0 + \frac{Q_0}{\sqrt{\pi a(t)}} \exp(-\frac{x^2}{a(t)})] \quad (6)$$

$$a(t) = \frac{w(t)^2}{2}, \quad A(t) = \exp(-\frac{t}{\tau})$$

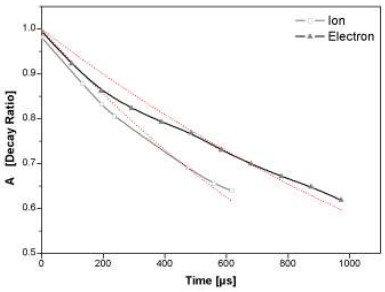

Fig. 6 Temporal change of A (decay ratio) and exponentially fitted curve of pure MgO.

The decay time constants of surface charge of ion and electron on pure MgO were calculated by describing the temporal variation of A and fitting exponentially as Fig. 6. Therefore, the decay time constants of pure MgO are as follows:

$$y = \exp(-\frac{t}{0.001891}), \qquad \tau_{ELEC} = 1891\mu s$$

$$y = \exp(-\frac{t}{0.001266}), \qquad \tau_{ION} = 1266\mu s$$

3.3 Characteristics as different types of MgO

We compared the diffusion and decay characteristics of three different types of MgO. Table I shows the diffusion coefficients and decay time constants of different sorts of MgO through procedure mentioned.

TABLE I. Decay time constants and diffusion coefficients as types of MgO

	Ion		Electron	
	Decay const. (μs)	Diffusion Coeff. (m^2/sec)	Decay const. (μs)	Diffusion Coeff. (m^2/sec)
Pure MgO	1266	6.80×10^{-6}	1891	9.12×10^{-5}
MgO1	1559	4.31×10^{-5}	1040	3.38×10^{-5}
MgO2	4151	2.26×10^{-4}	2621	4.71×10^{-4}

In order to see the tendency simultaneously, Fig. 7 describe diffusion coefficient and decay speed (1/τ) as different kinds of MgO. In notable characteristics, despite the slowest decay speed of electron and ion surface charge, MgO2 had the fastest diffusion speed. On the other hand, despite the slowest diffusion speed of electron surface charge, MgO1 had the fastest decay speed. We could decide that diffusion speed and decay speed had opposite tendency while comparing with relative speed between decay and diffusion among different types of MgO. Even though we observed relative relations between decay and diffusion speed as different types MgO, it is necessary to calculate accurate portions of decrement separately by decay and diffusion in the decrement of total peak density. Table II describes decrement ratio by decay and diffusion with the polarity of surface charge.

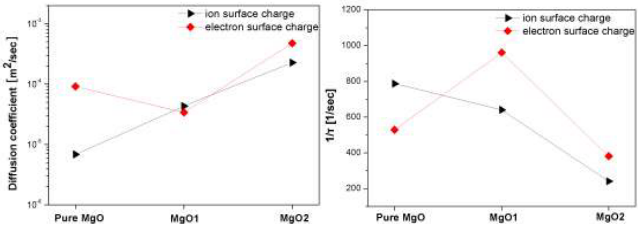

Fig. 7 Diffusion coefficients and Decay speed(1/τ) as three types of MgO.

Table II. shows the decrement ratio of total peak density from initial total peak density, σ_i. In Table II. the σ_i and σ_f present initial total peak density and final total peak density after taking about 1ms, respectively. The final total peak density on pure MgO was 0.456 rates of initial value, that on MgO1 was 0.537 rates and that on MgO2 was 0.569 rates. In Table II. , σ_{decay} and σ_{diff} present the decrement of peak density by pure decay and by pure diffusion, after taking about 1ms, respectively. It is evident that the decrement of electron surface density is bigger than that of ion surface density in common just by considering the polarity of surface charge each MgO. In short, the decrement of electron surface density was dominant factor in the decrement of total surface density regardless of types of MgO. However, the decrement of ion surface density was an important factor to generate the difference of the decrement of total surface density as different kinds of MgO. From Table II. the range of gap of electron's final density among different types of MgO was 0.01~0.046 and that of ion's was 0.022~0.066.

TABLE II. Decrement portion by diffusion and decay with the polarity of surface charge

	Pure MgO		MgO1		MgO2	
	Ion	Electron	Ion	Electron	Ion	Electron
$\sigma_{decay} / \sigma_i$	0.124	0.065	0.087	0.162	0.056	0.076
σ_{diff} / σ_i	0.127	0.227	0.120	0.094	0.129	0.170
$(\sigma_{diff} + \sigma_{decay}) / \sigma_i$	0.251	0.292	0.207	0.256	0.185	0.246
σ_f / σ_i	0.456		0.537		0.569	

On the contrary, although the portion of decrement of ion surface density in total decrement was lower, the difference of ion's final density among different types of MgO was distinctly different in Table II. Moreover, the major factor of decrement of ion's density was obviously the decay regardless of the decrement by pure diffusion described in Table II. In this research, the more co-doping with additional material, the slower decay speed of ion surface density. Hence, the difference of decrement rate of total surface charge was mainly affected by the decay speed of ion surface charge as different types of MgO.

Fig. 8 shows the address and sustain voltage margins of test panels, where the full driving waveform for different scanning times of 30μs and 1ms at 400Torr Ne-Xe(4%). The test panel both MgO1 and MgO2 had the extended voltage margins than pure MgO, while applying addressing discharge at 1ms after the ramp reset, the voltage margin with pure MgO is more diminished than any other MgO.

Table III shows address delay time for each MgO. The address delay time of MgO1 was the fastest, but that of MgO2 was slowest. It was already reported that when we doped Sc on MgO, the address delay time improved but wall charge is less collected in MgO surface and also made co-doping some material such as Ca, Al, Si to solve the wall charge loss. [5]-[6] In this work, when we doped Sc on MgO, the surface charge loss due to increasing surface conductivity was compensated by first co-doping with Al. However, in spite of fairly decreasing the decay loss of ion surface charge, additional co-doping with Ca deteriorated the address delay time. Consequently, doping with Sc and co-doping with Al was a good method to satisfy both improving address delay time and surface charge loss, simultaneously.

Table III. Address delay time of test panel for each MgO

	Delay Time(nsec)		
	$T_f + T_S$	T_S	T_f
Pure MgO	1344	324	1020
MgO1	1226	246	980
MgO2	1449	409	1040

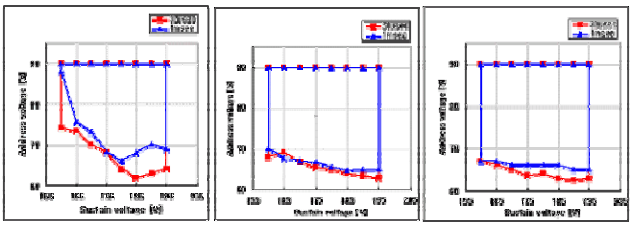

(a) (b) (c)

Fig. 8 Full driving voltage margin for each MgO with different scanning time: (a) pure MgO, (b) MgO1, and (c) MgO2.

4. Summary

We have investigated the diffusion coefficients and decay time constants as different types of doped MgO from the measurement of the surface charge distribution using electro optic effect of BSO crystal. It was found that the decay speed and diffusion speed had relatively opposite tendency. Moreover, it was concluded that the decrement of electron surface charge density was the dominant factor in the total surface charge variation regardless of types of MgO. On the other hand, the decrement of ion surface charge density especially pure decay loss led to make difference in that of total surface density as different kinds of MgO. MgO doped with Sc and co-doped with Al showed the fastest address delay time and less surface charge loss.

5. Reference

[1] K. H. Park, and Y. S. Kim, IMID'06, pp375-378, (2006)
[2] C. H. Ha, J. K. Kim, and K. W. Whang, IMID'07, pp1391-1394, (2007).
[3] D. C. Jeong, H. S. Bae, and K. W. Whang, *J. Appl. Phys*., vol. 97, pp. 013 304-1_031 304-8, Jan. 2005
[4] David A. Porter and Kenneth E. Easterling, *Phase Transfromations in Metal and Alloys*, Van Nostrand Reinhold Company, 1981.
[5] Harm Tolner, IDW'06, pp.333-336 (2006)
[6] Choi, Jeong Sik, European Patent, 1679732, 2006